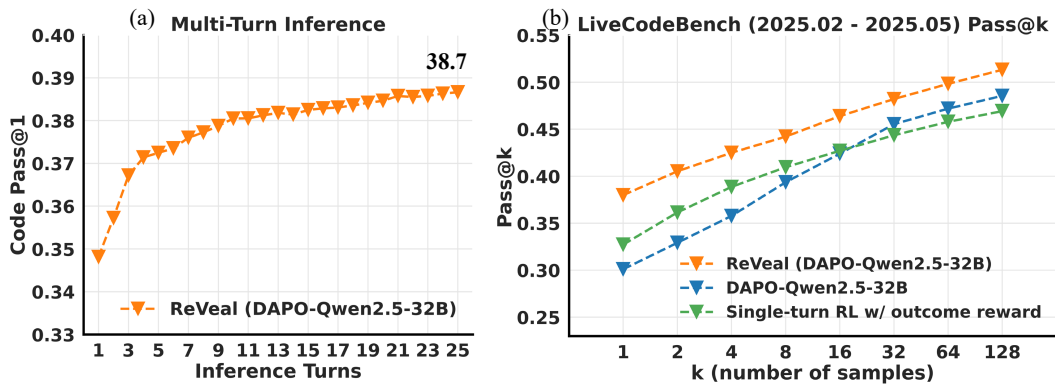


000 001 002 003 004 005 REVEAL: SELF-EVOLVING CODE AGENTS VIA 006 RELIABLE SELF-VERIFICATION 007 008 009

010 **Anonymous authors**
011 Paper under double-blind review
012
013
014
015
016
017
018
019
020
021
022
023
024
025
026

ABSTRACT

011 Reinforcement learning with verifiable rewards (RLVR) has advanced the rea-
012 soning capabilities of large language models. However, existing methods rely
013 solely on outcome rewards, without explicitly optimizing verification or leveraging
014 reliable signals from realistic environments, leading to unreliable self-verification
015 and limited test-time scaling. To address this, we widen the verification-generation
016 asymmetry by explicitly optimizing self-verification, making it a reliable driver
017 of deeper test-time scaling. We introduce *ReVeal*, a multi-turn *Reinforcement*
018 learning framework that evolves code generation through self-*Verification* and
019 tool-based *evaluation*. ReVeal structures long-horizon reasoning as iterative gener-
020 ation-verification turns and incorporates TAPO for turn-level credit assignment,
021 fostering the co-evolution of code and test generation. At inference, this strength-
022 ened self-verification enables the model to use self-constructed tests and tool
023 feedback to continuously evolve code for **20+** turns on LiveCodeBench despite
024 training on only three. It also significantly improves *Pass@k*, indicating stronger
025 exploration that expands the reasoning boundaries of the base model. These find-
026 ings highlight the promise of ReVeal as a scalable paradigm for RL training and
027 test-time scaling, paving the way for more robust and autonomous AI agents.
028



041 Figure 1: Performance of ReVeal on LiveCodeBench V6. (a) ReVeal enables effective test-time
042 scaling, with Pass@1 accuracy improving from 34.8% at turn 1 to 38.7% at turn 25. (b) ReVeal
043 (max_turn=10) consistently outperforms both the base model and the RL baseline in Pass@k,
044 expanding the base model’s reasoning boundaries, which the RL baseline fails to achieve.
045

1 INTRODUCTION

048 Reinforcement learning with verifiable rewards (RLVR) has recently shown strong potential to
049 enhance the reasoning abilities of large language models (LLMs) (DeepSeek-AI et al., 2025; OpenAI).
050 A key factor behind this success is the emergence of reflection and self-verification, which allow
051 models to iteratively refine their reasoning. Recent analyses identify the *verification-generation*
052 *asymmetry* (i.e., easier to verify than to solve) as the underlying mechanism for these improvements
053 and a key driver of test-time scaling (Wei, 2025; Setlur et al., 2025). However, current RLVR methods
054 rely solely on outcome rewards without explicitly optimizing verification. This leads to unreliable

054 self-verification, where models often produce verbose, uninformative reflections or random guessing
 055 on hard problems, and limits the effectiveness of test-time scaling: prior studies show that reasoning
 056 performance plateaus once test-time compute exceeds the training horizon (Setlur et al., 2025).
 057

058 Complex problem-solving, such as competitive programming, typically requires multiple iterations
 059 of verification and revision rather than being solved in a single attempt, making accurate feedback
 060 essential to guide refinement. This highlights the need for verification-driven multi-turn reasoning.
 061 Prior work has attempted this either by training a separate critic model to assess each attempt—without
 062 leveraging tool feedback and at the cost of added inference-time complexity (Xie et al., 2025)—or by
 063 relying on execution feedback against pre-existing public tests, which are rarely available in real-world
 064 scenarios (Gehring et al., 2025). As a result, these methods provide limited and non-generalizable
 065 verification, leaving self-verification unreliable and limiting sustained improvement.

066 To address these limitations, we propose **Re-
 067 Veal**, a multi-turn RL framework that *explicitly optimizes self-verification*, thereby widening
 068 the verification-generation (V-G) asymmetry and fostering co-evolution of both capabili-
 069 ties during training. This enables models at
 070 inference to obtain reliable verification signals
 071 from realistic environments and iteratively re-
 072 fine their solutions, without needing to rely on
 073 pre-existing tests. The widened V-G gap allows
 074 verification to drive sustained improvements in
 075 generation, ultimately enabling deeper test-time
 076 scaling (Figure 2).
 077

078 Concretely, ReVeal structures long-horizon reasoning into iterative generation and verification turns.
 079 At each turn, the model generates candidate code and *self-verifies* its correctness by constructing test
 080 cases and invoking external tools (e.g., a Python interpreter) for execution. This closed loop yields
 081 actionable verification signals and fine-grained feedback, allowing the model to identify errors, revise
 082 strategies, and progressively refine its output across turns. For training, we attach *dense, turn-level*
 083 *rewards* that directly supervise both code quality and verification accuracy. To ensure robustness,
 084 ReVeal employs a *Turn-Aware Policy Optimization (TAPO)* tailored for the generation-verification
 085 interplay, assigning credit at the turn granularity and preventing reward gaming (e.g., generating trivial
 086 code to hack verification rewards). Unlike outcome-only RL methods, ReVeal makes verification
 087 itself an optimization target, turning verification signals into reliable drivers of improvement.

088 We evaluate ReVeal on the challenging LiveCodeBench benchmark (Jain et al., 2024). Notably,
 089 despite being trained on only three reasoning turns, ReVeal sustains continuous refinement for over
 090 20+ inference turns, showing robust extrapolation beyond its training horizon and tackling problems
 091 previously unsolved. Furthermore, ReVeal significantly outperforms the base model in Pass@k by
 092 leveraging verification signals and tool feedback to guide more effective exploration, achieving an
 093 expansion of the underlying model’s reasoning boundaries that standard RL methods fail to reach.
 094 These results validate ReVeal as not only a practical framework for self-evolving code agents, but
 095 also as a general RL paradigm for tasks with verification-generation asymmetry, where explicitly
 096 optimizing verification unlocks reliable long-horizon reasoning.

097 2 METHODS

100 2.1 REVEAL FRAMEWORK

101 2.1.1 ITERATIVE GENERATION–VERIFICATION LOOP

103 ReVeal organizes long-horizon reasoning into an interleaved *generation-verification* loop with tool
 104 execution feedback, where verification itself is explicitly optimized to provide reliable signals for
 105 multi-turn refinement. As illustrated in Figure 3, we use a single policy for both generation and
 106 verification to reduce system complexity and cost and to enable cross-capability transfer, so that
 107 solutions and their verification strategies co-evolve under a shared training scheme. In the code-
 108 generation setting, *generation* produces candidate code, whereas *verification* synthesizes and executes

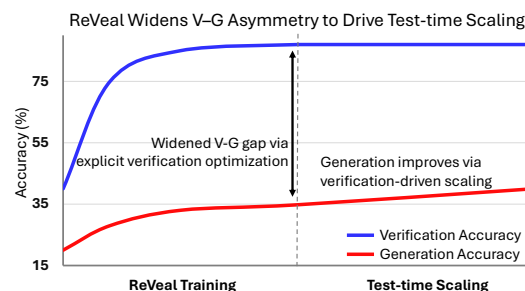


Figure 2: ReVeal expands the V-G gap.

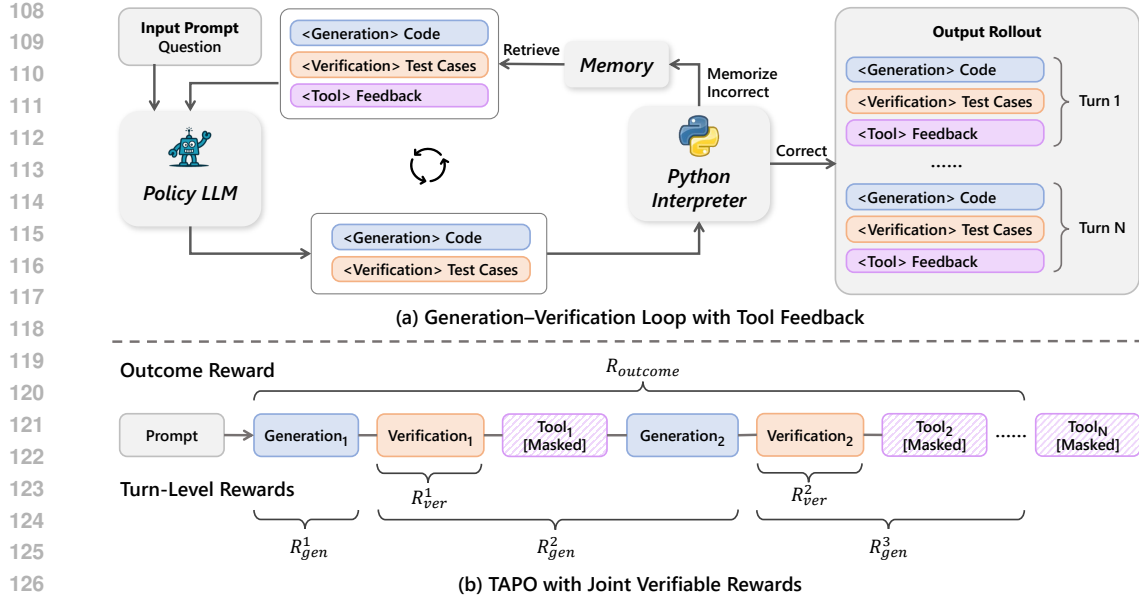


Figure 3: Illustration of ReVeal. (a) Iterative generation-verification loop with tool feedback. (b) TAPO with joint verifiable rewards: outcome, generation, and verification rewards.

tests to assess correctness. Fine-grained feedback from tool execution (e.g., Python interpreter) is appended to the rollout and conditions the next turn. The loop continues until a valid solution is found or a turn budget K is reached, enabling progressive refinement without external critics or predefined test cases.

Table 4 illustrates a multi-turn rollout under ReVeal’s structured prompting, which decouples generation, verification, and tool feedback into distinct segments. At each turn, the policy first reasons thoroughly and explores diverse reasoning patterns freely, then emits structured outputs: executable code in `<generation-answer>` and executable tests in `<verification-answer>`. As shown in the case study, after producing candidate code the model begins verification: it hypothesizes potential failure modes and edge conditions to propose diverse test cases. The `<tool-feedback>` section then records execution results, including runtime errors, invalid test cases, as well as the expected output, actual output, and pass/fail judgment for each valid test case. Based on this feedback, the model interprets traces and error messages, diagnoses underlying causes, and adjusts both its candidate code and its verification plan in the next turn. Full prompting and feedback templates are provided in Tables 5 and 6.

2.1.2 TOOL-AUGMENTED VERIFICATION

The interaction with external tools provides reliable, fine-grained supervisory signals that condition subsequent reasoning and enable systematic refinement of both code and verification strategies across turns. More importantly, tool interaction broadens exploration during reinforcement learning by revealing concrete failure modes, steering the policy into promising regions of the search space beyond a single attempt and helping it escape local optima. Empirically (see §3.3), this yields consistently higher pass@ k than the base model.

During RL training, the `<tool-feedback>` section is excluded from the loss and used only as contextual input, which stabilizes optimization while preserving coherent multi-turn rollouts. To ensure feedback quality during training, we adopt a filtering mechanism: model-generated test cases are executed on candidate code only if they are verified against a golden solution. This guarantees that execution traces provide legitimate supervision, thereby improving feedback precision and guiding exploration toward correct solutions. At test time, no golden reference is available; all generated test cases are executed, making verification fully autonomous. This places a strong demand on the model’s ability to generate high-quality tests. To meet this demand, ReVeal adopts a novel RL algorithm that incentivizes diverse and reliable test construction.

162
163

2.2 TURN-AWARE RL FOR THE GENERATION-VERIFICATION PARADIGM

164
165
166
167
168
169
170
171

Prior RLVR methods rely on outcome-only signals to optimize an entire long reasoning trace, but this provides imprecise credit to intermediate verification and often degenerates into blind reflection. Yet one may ask: *can the current paradigm fully sustain reliable verification and deeper test-time scaling?* Verification, however, is a non-trivial task: with well-designed verifiable rewards, a task can often be solved effectively. This motivates ReVeal to explicitly optimize verification with hard-to-hack rewards, which widen the verification-generation gap. At test time, this asymmetry becomes an asset: easier and more reliable verification signals can effectively guide the harder generation process to evolve over many turns.

172
173

2.2.1 JOINT VERIFIABLE REWARDS

174
175
176
177

To jointly train generation and verification, ReVeal decomposes the reward into three complementary components (Fig. 3b): an *outcome reward* supervising the final solution, a *generation reward* capturing improvements across generation turns, and a *verification reward* evaluating the quality of generated tests. This design naturally links the two roles in a co-evolutionary loop.

178
179
180

Outcome reward. The outcome reward shapes the entire reasoning chain by the final solution quality:

181

$$r_{\text{outcome}} = r_{\text{format}} + r_{\text{passrate}}, \quad (1)$$

182
183

where the format reward r_{format} ensures that the model produces well-formed generation and verification blocks,

184
185
186

$$r_{\text{format}} = \begin{cases} 1, & \text{if the output format is correct,} \\ -1, & \text{otherwise,} \end{cases} \quad (2)$$

187
188
189
190
191

and $r_{\text{passrate}} = 5 \times \text{passrate}$ measures final code accuracy with $\text{passrate} \in [0, 1]$, giving $r_{\text{outcome}} \in [-1, 6]$. The format reward ensures that the output follows the prescribed generation-turn and verification-turn tags, so that we can reliably identify each turn and assign the correct turn-level reward, and that the code and test-case blocks satisfy the required format, allowing us to reliably extract code and tests for tool execution.

192
193

Generation reward. For each generation turn k (odd), we compute the pass rate r_{passrate}^k of the code produced and define:

194
195
196
197

$$r_{\text{gen}}^k = \begin{cases} r_{\text{passrate}}^1, & k = 1, \\ \text{abs} \cdot r_{\text{passrate}}^k + \text{imp} \cdot (r_{\text{passrate}}^k - r_{\text{passrate}}^{k-2}), & k \geq 3, \end{cases}$$

198
199
200
201
202

where abs and imp weight absolute accuracy and iterative improvement. We set $\text{abs} = 0$, $\text{imp} = 1$ so that the reward encourages real improvements in code accuracy across turns.

203
204
205

Verification reward. For each verification turn k (even), we reward the proportion of generated tests that succeed when executed on a golden code:

206
207
208
209
210
211

$$r_{\text{ver}}^k = \frac{\#\{\text{test cases in turn } k \text{ that pass}\}}{\#\{\text{test cases generated in turn } k\}}. \quad (3)$$

2.2.2 TURN-AWARE POLICY OPTIMIZATION

212
213
214
215

Preliminaries. Our algorithm builds on the Proximal Policy Optimization (PPO) framework (Schulman et al., 2017), an on-policy actor-critic method that optimizes a clipped surrogate objective for stable updates. PPO typically estimates token-level advantages using Generalized Advantage Estimation (GAE) (Schulman et al., 2018):

$$\hat{A}_t^{\text{GAE}(\gamma, \lambda)} = \sum_{l=0}^{\infty} (\gamma \lambda)^l (r_{t+l} + \gamma V_{t+l+1} - V_{t+l}), \quad (4)$$

where $\gamma \in [0, 1]$ is the discount factor and $\lambda \in [0, 1]$ controls the bias-variance trade-off.

216 **Turn-Aware Policy Optimization.** Building on our structured reward design, we introduce *Turn-*
 217 *Aware Policy Optimization* (TAPO), which preserves the PPO actor-critic framework but only **modifies**
 218 **the advantage estimator: instead of the standard GAE-based advantages, TAPO uses a turn-aware**
 219 **return to construct the advantage estimates.** TAPO leverages the critic to efficiently bootstrap from
 220 both token-level Monte Carlo returns and turn-level returns, enabling stable learning across these two
 221 reward granularities.

222 **1. Token-level return.** We set $\lambda = 1$ and $\gamma = 1$ (pure Monte Carlo). **For a response of length T , we**
 223 **define the token-level rewards as $r_T = r_{\text{outcome}}$ and $r_t = 0$ for all $t < T$.** For token step t :

$$225 \quad R_t = \sum_{l=0}^{T-t} r_{t+l} = r_t + R_{t+1}, \quad R_{T+1} = 0. \quad (5)$$

226 **2. Turn-level return.** To mitigate adversarial reward gaming (e.g., generating trivial code that
 227 hacks the verification reward), we introduce a *turn-level* return tailored to the generation-verification
 228 interplay. Specifically, (i) each generation reward is assigned both to its own generation turn and to
 229 the immediately preceding verification turn, and (ii) each verification reward is confined strictly to
 230 its own verification turn. This design prevents reward hacking by ensuring that generation turns are
 231 rewarded solely based on code quality, rather than verification success. Let $\{t_1, \dots, t_K\}$ denote the
 232 token indices at which each turn ends (alternating generation and verification), and define:
 233

$$235 \quad R^{\text{turn}}(t_k) = \begin{cases} r_{\text{gen}}^k, & \text{if turn } k \text{ is generation,} \\ r_{\text{ver}}^k + R^{\text{turn}}(t_{k+1}), & \text{if turn } k \text{ is verification,} \end{cases} \quad R^{\text{turn}}(t_{K+1}) = 0. \quad (6)$$

236 For token t , let $\tau(t) = \min\{t_k \mid t_k \geq t\}$ and define

$$239 \quad R_t^{\text{turn}} = \begin{cases} R^{\text{turn}}(\tau(t)), & \text{if } \tau(t) \text{ exists,} \\ 0, & \text{otherwise.} \end{cases} \quad (7)$$

240 **3. Turn-aware return.** The final return combines the two levels:

$$243 \quad \tilde{R}_t = R_t + R_t^{\text{turn}}, \quad A_t = \tilde{R}_t - V_t, \quad (8)$$

244 where V_t is the critic model’s estimate at step t . These advantages A_t then replace the standard GAE
 245 estimates in the PPO objective, completing the TAPO update.

246 **Discussion.** TAPO provides sharper supervision than outcome-only methods by explicitly assigning
 247 credit at both token and turn levels. It integrates outcome rewards, which keep the process aligned
 248 with final correctness, and turn-level signals, which provide dense supervision for progressive
 249 refinement. This structure establishes a feedback loop: stronger tests expose errors that drive code
 250 improvements, which are then reinforced by the generation reward, while improved code raises the
 251 bar for verification, pushing the model to generate richer and more challenging tests. By design,
 252 TAPO prevents reward gaming and turns this loop into stable co-evolution of code and tests. Crucially,
 253 TAPO is a *general* credit-assignment algorithm, applicable to any reasoning task with verifiable
 254 rewards for both generation and verification.

256 3 EXPERIMENTS

258 3.1 SETTINGS

260 **Dataset** We construct our training dataset from TACO (Li et al., 2023), a large-scale corpus
 261 comprising 26,443 algorithmic programming problems sourced from competitive programming
 262 platforms such as LeetCode (LLC, 2015) and Codeforces (Codeforces, 2025). Each problem consists
 263 of a natural language description, golden solutions, and multiple test cases.

264 To address noise in the raw dataset, we first filter out problems containing unsupported content types,
 265 specifically those tagged with interactive or image elements. To ensure testability and correctness,
 266 we process two types of test case format, function-based tests and standard input/output tests, into a
 267 unified structure compatible with our code execution environment. We then execute each test case
 268 against the first available golden solution in our execution environment. Problems where the golden
 269 code fails to pass all associated test cases are discarded. After preprocessing, we retain a high-quality
 dataset of 11,151 problems for training and 509 problems for testing.

270
 271 Table 1: Performance comparison of ReVeal with baseline methods on LiveCodeBench V6 and
 272 CodeContests. Pass@1 indicates the success rate; Δ_{\uparrow} and Δ_{\downarrow} represent the percentages of incorrect
 273 solutions corrected and correct solutions degraded after revision, respectively.

| 274 275 276 277 278 279 280 281 282 283 284 285 286 287 288 289 290 291 292 293 294 295 296 297 298 299 300 301 302 303 304 305 306 307 308 309 310 311 312 313 314 315 316 317 318 319 320 321 322 323 | 274 275 276 277 278 279 280 281 282 283 284 285 286 287 288 289 290 291 292 293 294 295 296 297 298 299 300 301 302 303 304 305 306 307 308 309 310 311 312 313 314 315 316 317 318 319 320 321 322 323 | | | 274 275 276 277 278 279 280 281 282 283 284 285 286 287 288 289 290 291 292 293 294 295 296 297 298 299 300 301 302 303 304 305 306 307 308 309 310 311 312 313 314 315 316 317 318 319 320 321 322 323 | | | |
|------------------------------------------------------------------------------------------------------------------------------------------------------------------------------------------------------------------------------------------------------------------------------------------------------------------------------------------------------------|------------------------------------------------------------------------------------------------------------------------------------------------------------------------------------------------------------------------------------------------------------------------------------------------------------------------------------------------------------|-------------|---------------------|------------------------------------------------------------------------------------------------------------------------------------------------------------------------------------------------------------------------------------------------------------------------------------------------------------------------------------------------------------|--------------|---------------------|-----------------------|
| | Model | Pass@1 | Δ_{\uparrow} | Δ_{\downarrow} | Pass@1 | Δ_{\uparrow} | Δ_{\downarrow} |
| <i>Existing Baselines</i> | | | | | | | |
| Qwen2.5-32B-Instruct | 24.8 | - | - | 13.3 | - | - | |
| DAPO-Qwen2.5-32B | 31.1 | - | - | 18.5 | - | - | |
| Qwen2.5-Coder-32B-Instruct | 29.5 | - | - | 14.6 | - | - | |
| w/ critic $\times 5$ Qwen2.5-Coder | 29.6 | 2.14 | 3.04 | - | - | - | |
| w/ critic $\times 5$ GPT-4o | 32.9 | 4.82 | 2.50 | - | - | - | |
| w/ critic $\times 5$ CTRL | 33.4 | 3.75 | 0.89 | - | - | - | |
| <i>RL based on DAPO-Qwen2.5-32B</i> | | | | | | | |
| Single-turn RL | 32.8 | - | - | 21.0 | - | - | |
| ReVeal $\times 25$ | 38.7 | 7.50 | 0.0 | 33.6 | 15.69 | 0.0 | |
| <i>Ablation Study: TAPO with Joint Verifiable Rewards</i> | | | | | | | |
| ReVeal $\times 8$ w/ outcome reward | 36.1 | 4.69 | 1.32 | 27.4 | 9.24 | 2.36 | |
| ReVeal $\times 8$ w/ TAPO with joint rewards | 37.7 | 5.62 | 0.0 | 30.4 | 12.30 | 0.0 | |

292 **Models and Training Details** We adopt DAPO-Qwen-32B (Yu et al., 2025) as our base model,
 293 which is reinforced with mathematical data, and we continue RL training on code datasets to adapt
 294 its reasoning capabilities to coding tasks. Our models are trained using Verl (Sheng et al., 2024)
 295 framework on 8/16 AMD Mi300x GPUs. The RL training process follows the hyperparameter
 296 settings listed in Table 2. We set maximum turns to 3 during RL training.

297 **Evaluation** We evaluate ReVeal on two code-generation benchmarks: LiveCodeBench (LCB) V6
 298 (2025.02–2025.05) (Jain et al., 2024) and CodeContests (Li et al., 2022). The evaluation process
 299 follows the hyperparameter configuration specified in Table 3. Although training is performed with a
 300 maximum of 3 turns, we evaluate the model under extended turn settings (8 and 25 turns) to assess its
 301 generalization to longer reasoning horizons and test-time scaling performance.

302 We use Pass@1 to measure the success rate of the model’s final code solutions. To evaluate the model’s
 303 verification and self-correction capabilities, we introduce two additional metrics: Δ_{\uparrow} denotes the
 304 fraction of initially incorrect solutions that become correct after revision, and Δ_{\downarrow} denotes the fraction
 305 of initially correct solutions that become incorrect after revision. In line with recent work (Yue et al.,
 306 2025), we use Pass@k up to $k = 128$ to assess whether ReVeal can push the reasoning boundaries
 307 beyond the base model, with at most 10 generation–verification turns per example.

309 **Memory Mechanism for Context Management** To improve inference efficiency under extended
 310 multi-turn rollouts, we use a short-term memory mechanism that retains only the last three turns as
 311 context, which prevents excessive context growth without hurting accuracy (detail in Appendix B.4).

313 **Code Execution Tool** We use Code Judge¹ as our code execution environment. Code Judge supports
 314 both function-based and standard input-output test case formats through a consistent interface.
 315 Designed for scalability and robustness, it enables efficient long-batch execution through multi-
 316 processing and provides reliable code evaluation.

318 **Baselines** We compare ReVeal against following baselines: (1) *Base*: base models without
 319 code-specific RL training; (2) *CTRL* (Xie et al., 2025) + *Qwen2.5-Coder-32B-Instruct*: five-turn
 320 critic–revision with a dedicated critic model; results cited from the original paper (evaluated on
 321 LCB 24.08–24.11); (3) *Single-turn RL with outcome reward*: RL with outcome-only rewards under
 322 standard <think>–<answer> prompting template without any external tool calls.

323 ¹<https://github.com/0xWJ/code-judge>

324
325

3.2 MAIN RESULTS

326
327
328
329
330
331
332

Table 1 shows that single-turn RL (outcome-only, no explicit optimization of self-verification or tool use) improves Pass@1 over the base models. ReVeal goes further by explicitly optimizing verification and enabling deeper inference, it surpass the single-turn RL baseline by a wide margin. Beyond deeper-turn gains, ReVeal also achieves higher Pass@1 at turn 1 (34.8%) than the single-turn RL baseline under equal inference budget on LCB V6, indicating that multi-turn training (3 turns) transfers exploration benefits into a stronger policy and that increasing training depth may further amplify gains.

333
334
335
336
337
338
339

ReVeal significantly outperforms critic-based methods such as CTRL. While critic models tailored for code tasks can be paired with policy models for multi-turn critique and revision, ReVeal employs a single policy model that self-verifies and iteratively refines its own outputs, yet achieves superior results, highlighting the benefit of jointly optimizing generation and verification. Specifically, ReVeal attains larger correction rates with near-zero degradation, demonstrating highly robust and reliable capabilities in self-verification, critique, and revision. (CTRL numbers are cited from earlier LCB version; see Table 7 for a V5 comparison on Qwen2.5-32B-Instruct.)

340
341
342
343

Ablation studies confirm the benefit of TAPO with joint verifiable rewards: at the same turn budget it yields higher Pass@1, increases Δ_{\uparrow} , and suppresses Δ_{\downarrow} compared to outcome-only training. In contrast, outcome-only rewards exhibit higher Δ_{\downarrow} , indicating that insufficiently optimized verification can drive incorrect revisions.

344
345
346
347
348
349
350
351
352

More Experiments To validate effectiveness and scalability across models, we evaluate ReVeal on another base model, Qwen2.5-32B-Instruct. The detailed results are in Appendix Table 7 and Figure 5. ReVeal outperforms single-turn RL baseline by 4.1%, which demonstrates the effectiveness of ReVeal. To demonstrate that the performance improvements are statistically significant, we repeated the experiment 8 times and reported the $mean \pm std$ in the Appendix Table 8. Across models of varying capability, ReVeal remains effective. With the stronger DAPO-Qwen2.5-32B backbone, ReVeal unlocks greater headroom: accuracy continues to improve with deeper inference turns and surpasses outcome-only RL by a wider margin. This underscores ReVeal’s potential on stronger backbones.

353
354
355
356
357

To verify that the performance improvements originate from explicit optimization rather than mere tool use, we conduct comparative experiments with ReAct prompting (Shinn et al., 2023), showing that ReVeal significantly outperforms ReAct across all turn budgets. Without explicit optimization for verification, ReAct fails to sustain effective deep multi-turn refinement. See Table 10 for details.

358
359

3.3 ANALYSIS

360
361
362
363
364
365
366
367
368
369
370

ReVeal Enables Test-time Scaling into Deeper Inference Regimes. As shown in Figure 1 (a), ReVeal enables effective test-time scaling through iterative generation and verification. Although the model is trained with a maximum of three reasoning turns, it continues to improve its solutions when more turns are allowed at inference time, leading to progressively higher code accuracy. For instance, Pass@1 increases from 34.8% at turn 1 to 36.7% at turn 3, and further rises to 38.7% by turn 25 for LiveCodeBench. This compellingly demonstrates how reliable self-verification and iterative environment feedback can enable compute scaling into deeper inference regimes, allowing ReVeal to solve previously intractable problems and evolve novel solutions. As a result, ReVeal supports self-improvement beyond the training horizon, enabling strong generalization in long-horizon reasoning during inference. Furthermore, these newly discovered solutions can be distilled back into the code LLM to further enhance its reasoning capabilities through continued training.

371
372
373
374
375
376
377

ReVeal Pushes Beyond the Reasoning Boundaries of the Base Model. We compare DAPO-Qwen2.5-32B and single-turn RL baseline with ReVeal using Pass@k metrics on LiveCodeBench. As shown in Figure 1 (b), the RL baseline outperforms the base model when $k < 32$, but its performance gain gradually diminishes as k increases. In contrast, ReVeal consistently outperforms both the base model and the RL baseline across all k values from 1 to 128, demonstrating its ability to surpass the reasoning boundaries beyond the base model. We attribute this improvement to ReVeal’s verification-driven exploration: tool-assisted verification provides targeted, execution-based feedback and precise judgments that guide the model to explore better solutions more effectively. With this enhanced

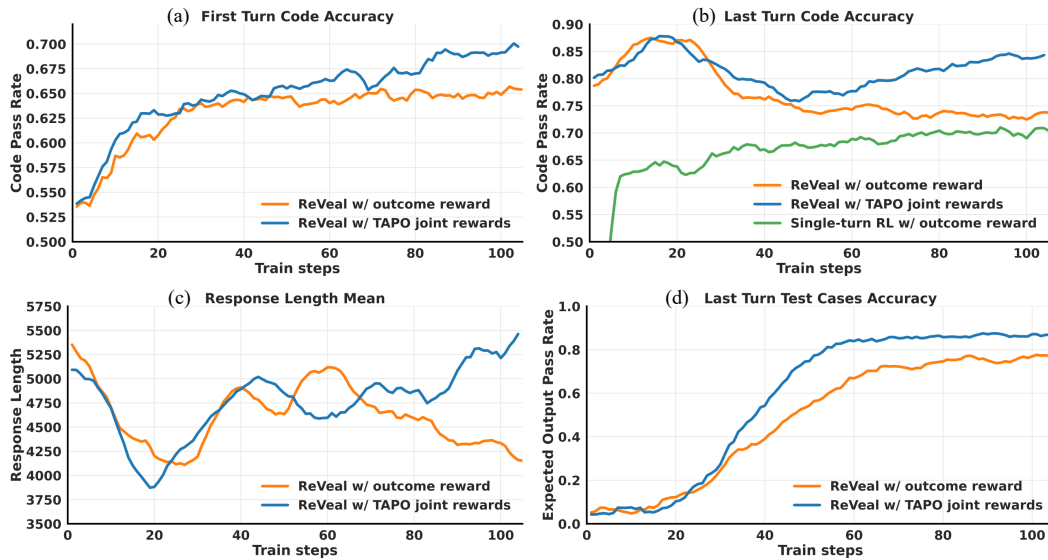


Figure 4: Training curves for (a) first-turn code accuracy, (b) last-turn code accuracy, (c) mean response length, and (d) last-turn test-case accuracy across three training methods. **Note on (b):** the dip before step 40 is due to expanded evaluation coverage: as format score reaches 0.9 around step 40, more problems enter the evaluation set, temporarily lowering accuracy.

exploration capability, the model continually self-evolves and grows beyond its initial reasoning capability during RL training. We believe this approach offers a promising path towards developing self-evolving agents with stronger reasoning capabilities.

Reveal Co-evolves the Model’s Generation and Verification Capabilities. Figure 4(b, d) illustrates the co-evolution of the model’s code and test case generation capabilities. As shown in Figure 4(b), once the format is learned, final code accuracy steadily improves during training and significantly surpasses the single-turn RL baseline. Moreover, comparing Figure 4(a) and (b) reveals that final solutions consistently outperform those generated at Turn 1, with the performance gap widening over time. This trend indicates that as the model’s verification ability strengthens, multi-turn refinement enables the exploration of better solutions, progressively enhancing its capacity to generate and refine code. After the format is learned, test-case accuracy rises substantially from about 50% at step 40 to nearly 88%, as shown in Figure 4 (d). Additionally, for correctly generated test cases, the model achieves over 85% accuracy in judging code correctness. This demonstrates that during inference, the model can reliably generate valid test cases and effectively leverage tool to produce accurate verification signals, which are critical for continuous improvements in code quality. These results provide strong evidence that Reveal jointly and effectively optimizes both generation and verification, enabling the model to evolve its reasoning capabilities throughout training.

The Effectiveness of TAPO with Joint Verifiable Rewards. As shown in Table 1, TAPO with joint rewards further enhances multi-turn performance compared to relying solely on outcome rewards. The training curves in Figure 4(a,b) show TAPO with joint rewards achieves more stable and consistent per-turn code gains, and Figure 4(d) shows it achieves higher test-case accuracy, indicating that explicitly optimizing verification yields higher-quality tests and more effective reasoning in code generation task. These benefits amplify in longer-sequence and harder verification scenarios. On the stronger DAPO-Qwen2.5-32B backbone with longer chains, dense turn-level supervision yields larger gains than on Qwen2.5-32B-Instruct with much shorter chains (see Table 7 and Figure 5). This is because outcome-only signals are too coarse for extremely long chains, providing imprecise credit to intermediate verification steps. Furthermore, in more challenging verification scenarios, such fine-grained supervision becomes increasingly essential, offering richer learning signals to enhance the model’s verification capabilities.

432

4 RELATED WORK

433

4.1 TOOL-AUGMENTED REASONING

436 Tool-integrated reasoning enables large language models (LLMs) to leverage external tools, such
 437 as search engines or code interpreters, to overcome inherent limitations in domain knowledge and
 438 mathematical operations. Early approaches demonstrated the benefits of tool integration via prompt
 439 engineering (Yao et al., 2023; Chen et al., 2023; Shinn et al., 2023) and supervised fine-tuning (Gou
 440 et al., 2024). ReAct (Yao et al., 2023) and Reflexion (Shinn et al., 2023), which interleave reasoning
 441 with acting or verbal self-critique to iteratively refine solutions under tool access. These approaches
 442 highlight the value of interactive signals, but they typically rely on prompt heuristics. More recently,
 443 multi-turn RL has been adopted to further enhance this capability on various reasoning tasks (Jin
 444 et al., 2025; Feng et al., 2025; Li et al., 2025). For example, Search-R1 (Jin et al., 2025) incorporates
 445 multi-turn interactions with a search engine to retrieve relevant contextual information during RL
 446 training. ReTool (Feng et al., 2025) and ToRL (Li et al., 2025) enable multi-turn code execution to
 447 support mathematical reasoning. Building on the promising potential of tool-integrated RL, Agent-
 448 R1 (Ouyang et al., 2025) introduces an open-source RL framework capable of supporting multi-turn,
 449 customization tool invocations.

450 Despite their effectiveness, most tool-augmented RL methods are predominantly outcome-driven: they
 451 rely on task success or failure as the sole training signal and do not explicitly optimize verification or
 452 assign credit across turns. Likewise, prompt-only agents lack turn-level, verifiable supervision, which
 453 can make self-verification unreliable on harder problems and limit sustained test-time improvement.
 454 Unlike prior tool-augmented works, ReVeal treats verification itself as a first-class optimization target
 455 alongside generation, and introduces Turn-Aware Policy Optimization rewards (TAPO) to provide
 456 fine-grained credit to both generation and verification turns. Our approach and prior tool-augmented
 457 methods are orthogonal and complementary, and can be naturally combined to further enhance
 458 reasoning capability.

459

4.2 SELF-VERIFICATION OF LLMs

460 Enabling LLMs to iteratively refine their outputs is critical for enhancing their reasoning capabilities.
 461 However, LLMs typically lack reliable self-judgment (Huang et al., 2024). One common solution
 462 is to introduce a separate critic model to verify the output of the policy model (Zhang et al., 2025;
 463 Xie et al., 2025). For example, CTRL (Xie et al., 2025) uses RL to train a critic model for code
 464 completion tasks. Although effective, these approaches incur the cost and complexity of maintaining
 465 and coordinating two distinct models.

466 An alternative strategy is to enable one single model to generate outputs and self-verify them. In
 467 mathematical reasoning, (Xiong et al., 2025) synthesizes long chains of thought that incorporate
 468 "self-reward" and "self-correction" signals as seed data for supervised fine-tuning, and then further
 469 enhances this ability via RL. In the code domain, execution feedback effectively verifies code
 470 correctness and provides useful information for fixing errors. RLEF (Gehring et al., 2025) performs
 471 multi-turn code generation and verification with an integrated code execution tool; however, it
 472 depends on publicly available test cases, limiting its applicability.

473 In contrast, ReVeal advances self-verification by having the model generate its own high-quality test
 474 cases on the fly. By explicitly crafting and executing these tests, ReVeal eliminates the dependency
 475 on pre-existing test suites and improves applicability to real-world software systems.

478

5 CONCLUSION

480 We presented REVEAL, a multi-turn reinforcement learning (RL) framework that makes verification a
 481 first-class optimization target alongside generation and organizes long reasoning chains into iterative
 482 generation–verification turns with tool feedback. Using TAPO with joint verifiable rewards, REVEAL
 483 equips LLMs with strong verification capabilities and demonstrates the surprising power of enabling
 484 code LLMs to self-evolve—both during RL training, where it pushes boundaries beyond the base
 485 model, and at test time, where multi-turn generation and verification continually refine outputs, even
 up to 20+ inference turns. This compellingly demonstrates that REVEAL can enable compute scaling

486 into deeper inference regimes, allowing it to solve previously intractable problems and evolve novel
487 solutions. Furthermore, these newly discovered solutions can be distilled back into the code LLM to
488 further enhance its reasoning capabilities through continued training.

489 Although we demonstrate REVEAL on code tasks, its general concept of generation–verification,
490 TAPO, and turn-level reward design can be applied to any domain with verifiable rewards for both
491 generation and verification and that exhibits verification asymmetry, offering a promising blueprint
492 for future advances in self-improving, more robust, and autonomous AI agents.

493

494

495

496

497

498

499

500

501

502

503

504

505

506

507

508

509

510

511

512

513

514

515

516

517

518

519

520

521

522

523

524

525

526

527

528

529

530

531

532

533

534

535

536

537

538

539

540 REFERENCES

541

542 Wenhui Chen, Xueguang Ma, Xinyi Wang, and William W. Cohen. Program of thoughts prompting:
 543 Disentangling computation from reasoning for numerical reasoning tasks, 2023. URL <https://arxiv.org/abs/2211.12588>.

544

545 Codeforces. Codeforces - competitive programming platform, 2025. URL <https://codeforces.com/>. Accessed: 2025-03-18.

546

547 DeepSeek-AI, Daya Guo, Dejian Yang, Haowei Zhang, Junxiao Song, Ruoyu Zhang, Runxin Xu,
 548 Qihao Zhu, Shirong Ma, Peiyi Wang, Xiao Bi, Xiaokang Zhang, Xingkai Yu, Yu Wu, Z. F. Wu,
 549 Zhibin Gou, Zhihong Shao, Zhuoshu Li, Ziyi Gao, Aixin Liu, Bing Xue, Bingxuan Wang, Bochao
 550 Wu, Bei Feng, Chengda Lu, Chenggang Zhao, Chengqi Deng, Chenyu Zhang, Chong Ruan,
 551 Damai Dai, Deli Chen, Dongjie Ji, Erhang Li, Fangyun Lin, Fucong Dai, Fuli Luo, Guangbo Hao,
 552 Guanting Chen, Guowei Li, H. Zhang, Han Bao, Hanwei Xu, Haocheng Wang, Honghui Ding,
 553 Huajian Xin, Huazuo Gao, Hui Qu, Hui Li, Jianzhong Guo, Jiashi Li, Jiawei Wang, Jingchang
 554 Chen, Jingyang Yuan, Junjie Qiu, Junlong Li, J. L. Cai, Jiaqi Ni, Jian Liang, Jin Chen, Kai Dong,
 555 Kai Hu, Kaige Gao, Kang Guan, Kexin Huang, Kuai Yu, Lean Wang, Lecong Zhang, Liang Zhao,
 556 Litong Wang, Liyue Zhang, Lei Xu, Leyi Xia, Mingchuan Zhang, Minghua Zhang, Minghui Tang,
 557 Meng Li, Miaojun Wang, Mingming Li, Ning Tian, Panpan Huang, Peng Zhang, Qiancheng Wang,
 558 Qinyu Chen, Qiushi Du, Ruiqi Ge, Ruisong Zhang, Ruizhe Pan, Runji Wang, R. J. Chen, R. L.
 559 Jin, Ruyi Chen, Shanghao Lu, Shangyan Zhou, Shanhua Chen, Shengfeng Ye, Shiyu Wang,
 560 Shuiping Yu, Shunfeng Zhou, Shuting Pan, S. S. Li, Shuang Zhou, Shaoqing Wu, Shengfeng
 561 Ye, Tao Yun, Tian Pei, Tianyu Sun, T. Wang, Wangding Zeng, Wanjia Zhao, Wen Liu, Wenfeng
 562 Liang, Wenjun Gao, Wenqin Yu, Wentao Zhang, W. L. Xiao, Wei An, Xiaodong Liu, Xiaohan
 563 Wang, Xiaokang Chen, Xiaotao Nie, Xin Cheng, Xin Liu, Xin Xie, Xingchao Liu, Xinyu Yang,
 564 Xinyuan Li, Xuecheng Su, Xuheng Lin, X. Q. Li, Xiangyue Jin, Xiaojin Shen, Xiaosha Chen,
 565 Xiaowen Sun, Xiaoxiang Wang, Xinnan Song, Xinyi Zhou, Xianzu Wang, Xinxia Shan, Y. K. Li,
 566 Y. Q. Wang, Y. X. Wei, Yang Zhang, Yanhong Xu, Yao Li, Yao Zhao, Yaofeng Sun, Yaohui Wang,
 567 Yi Yu, Yichao Zhang, Yifan Shi, Yiliang Xiong, Ying He, Yishi Piao, Yisong Wang, Yixuan Tan,
 568 Yiyang Ma, Yiyuan Liu, Yongqiang Guo, Yuan Ou, Yuduan Wang, Yue Gong, Yuheng Zou, Yujia
 569 He, Yunfan Xiong, Yuxiang Luo, Yuxiang You, Yuxuan Liu, Yuyang Zhou, Y. X. Zhu, Yanhong
 570 Xu, Yanping Huang, Yaohui Li, Yi Zheng, Yuchen Zhu, Yunxian Ma, Ying Tang, Yukun Zha,
 571 Yuting Yan, Z. Z. Ren, Zehui Ren, Zhangli Sha, Zhe Fu, Zhean Xu, Zhenda Xie, Zhengyan Zhang,
 572 Zhewen Hao, Zhicheng Ma, Zhigang Yan, Zhiyu Wu, Zihui Gu, Zijia Zhu, Zijun Liu, Zilin Li,
 573 Ziwei Xie, Ziyang Song, Zizheng Pan, Zhen Huang, Zhipeng Xu, Zhongyu Zhang, and Zhen
 574 Zhang. Deepseek-r1: Incentivizing reasoning capability in llms via reinforcement learning, 2025.
 575 URL <https://arxiv.org/abs/2501.12948>.

576

577 Jiazhan Feng, Shijue Huang, Xingwei Qu, Ge Zhang, Yujia Qin, Baoquan Zhong, Chengquan Jiang,
 578 Jinjin Chi, and Wanjun Zhong. Retool: Reinforcement learning for strategic tool use in llms, 2025.
 579 URL <https://arxiv.org/abs/2504.11536>.

580

581 Jonas Gehring, Kunhao Zheng, Jade Copet, Vegard Mella, Quentin Carbonneaux, Taco Cohen, and
 582 Gabriel Synnaeve. Rlef: Grounding code llms in execution feedback with reinforcement learning,
 583 2025. URL <https://arxiv.org/abs/2410.02089>.

584

585 Zhibin Gou, Zhihong Shao, Yeyun Gong, Yelong Shen, Yujiu Yang, Minlie Huang, Nan Duan, and
 586 Weizhu Chen. Tora: A tool-integrated reasoning agent for mathematical problem solving, 2024.
 587 URL <https://arxiv.org/abs/2309.17452>.

588

589 Jie Huang, Xinyun Chen, Swaroop Mishra, Huaixiu Steven Zheng, Adams Wei Yu, Xinying Song,
 590 and Denny Zhou. Large language models cannot self-correct reasoning yet, 2024. URL <https://arxiv.org/abs/2310.01798>.

591

592 Naman Jain, King Han, Alex Gu, Wen-Ding Li, Fanjia Yan, Tianjun Zhang, Sida Wang, Armando
 593 Solar-Lezama, Koushik Sen, and Ion Stoica. Livecodebench: Holistic and contamination free
 594 evaluation of large language models for code, 2024. URL <https://arxiv.org/abs/2403.07974>.

595

596 Bowen Jin, Hansi Zeng, Zhenrui Yue, Jinsung Yoon, Sercan Arik, Dong Wang, Hamed Zamani, and
 597 Jiawei Han. Search-r1: Training llms to reason and leverage search engines with reinforcement
 598 learning, 2025. URL <https://arxiv.org/abs/2503.09516>.

594 Rongao Li, Jie Fu, Bo-Wen Zhang, Tao Huang, Zhihong Sun, Chen Lyu, Guang Liu, Zhi Jin, and
 595 Ge Li. Taco: Topics in algorithmic code generation dataset, 2023. URL <https://arxiv.org/abs/2312.14852>.
 596

597 Xuefeng Li, Haoyang Zou, and Pengfei Liu. Torl: Scaling tool-integrated rl, 2025. URL <https://arxiv.org/abs/2503.23383>.
 598

600 Yujia Li, David Choi, Junyoung Chung, Nate Kushman, Julian Schrittweis, Rémi Leblond, Tom
 601 Eccles, James Keeling, Felix Gimeno, Agustin Dal Lago, Thomas Hubert, Peter Choy, Cyprien
 602 de Masson d'Autume, Igor Babuschkin, Xinyun Chen, Po-Sen Huang, Johannes Welbl, Sven Gowal,
 603 Alexey Cherepanov, James Molloy, Daniel Mankowitz, Esme Sutherland Robson, Pushmeet Kohli,
 604 Nando de Freitas, Koray Kavukcuoglu, and Oriol Vinyals. Competition-level code generation with
 605 alphacode. *arXiv preprint arXiv:2203.07814*, 2022.
 606

607 Jiawei Liu, Chunqiu Steven Xia, Yuyao Wang, and Lingming Zhang. Is your code generated by
 608 chatgpt really correct? rigorous evaluation of large language models for code generation. *Advances
 609 in Neural Information Processing Systems*, 36:21558–21572, 2023.
 610

611 LeetCode LLC. Leetcode: Online coding platform for technical interview preparation, 2015. URL
 612 <https://leetcode.com/>. Accessed: 2025-05-16.
 613

614 OpenAI. Learning to reason with llms.
 615 [urlhttps://openai.com/index/learning-to-reason-with-llms/](https://openai.com/index/learning-to-reason-with-llms/). Accessed: 15 March 2025.
 616

617 Jie Ouyang, Ruiran Yan, Yucong Luo, Mingyue Cheng, Qi Liu, Zirui Liu, Shuo Yu, and Daoyu
 618 Wang. Training powerful lilm agents with end-to-end reinforcement learning, 2025. URL <https://github.com/0russwest0/Agent-R1>.
 619

620 John Schulman, Filip Wolski, Prafulla Dhariwal, Alec Radford, and Oleg Klimov. Proximal policy
 621 optimization algorithms, 2017. URL <https://arxiv.org/abs/1707.06347>.
 622

623 John Schulman, Philipp Moritz, Sergey Levine, Michael Jordan, and Pieter Abbeel. High-dimensional
 624 continuous control using generalized advantage estimation, 2018. URL <https://arxiv.org/abs/1506.02438>.
 625

626 Amrith Setlur, Matthew Y. R. Yang, Charlie Snell, Jeremy Greer, Ian Wu, Virginia Smith, Max
 627 Simchowitz, and Aviral Kumar. e3: Learning to explore enables extrapolation of test-time compute
 628 for llms, 2025. URL <https://arxiv.org/abs/2506.09026>.
 629

630 Guangming Sheng, Chi Zhang, Zilingfeng Ye, Xibin Wu, Wang Zhang, Ru Zhang, Yanghua Peng,
 631 Haibin Lin, and Chuan Wu. Hybridflow: A flexible and efficient rlhf framework. *arXiv preprint
 632 arXiv:2409.19256*, 2024.
 633

634 Noah Shinn, Federico Cassano, Edward Berman, Ashwin Gopinath, Karthik Narasimhan, and Shunyu
 635 Yao. Reflexion: Language agents with verbal reinforcement learning, 2023.
 636

637 Jason Wei. Asymmetry of verification and the verifier's law. [https://www.jasonwei.net/
 638 blog/asymmetry-of-verification-and-verifiers-law](https://www.jasonwei.net/blog/asymmetry-of-verification-and-verifiers-law), 2025.
 639

640 Zhihui Xie, Jie chen, Liyu Chen, Weichao Mao, Jingjing Xu, and Lingpeng Kong. Teaching language
 641 models to critique via reinforcement learning, 2025. URL <https://arxiv.org/abs/2502.03492>.
 642

643 Wei Xiong, Hanning Zhang, Chenlu Ye, Lichang Chen, Nan Jiang, and Tong Zhang. Self-
 644 rewarding correction for mathematical reasoning, 2025. URL <https://arxiv.org/abs/2502.19613>.
 645

646 An Yang, Anfeng Li, Baosong Yang, Beichen Zhang, Binyuan Hui, Bo Zheng, Bowen Yu, Chang
 647 Gao, Chengan Huang, Chenxu Lv, Chujie Zheng, Dayiheng Liu, Fan Zhou, Fei Huang, Feng Hu,
 648 Hao Ge, Haoran Wei, Huan Lin, Jialong Tang, Jian Yang, Jianhong Tu, Jianwei Zhang, Jianxin
 649 Yang, Jiaxi Yang, Jing Zhou, Jingren Zhou, Junyang Lin, Kai Dang, Keqin Bao, Kexin Yang,
 650 Le Yu, Lianghao Deng, Mei Li, Mingfeng Xue, Mingze Li, Pei Zhang, Peng Wang, Qin Zhu, Rui
 651 Men, Ruize Gao, Shixuan Liu, Shuang Luo, Tianhao Li, Tianshi Tang, Wenbiao Yin, Xingzhang

648 Ren, Xinyu Wang, Xinyu Zhang, Xuancheng Ren, Yang Fan, Yang Su, Yichang Zhang, Yinger
 649 Zhang, Yu Wan, Yuqiong Liu, Zekun Wang, Zeyu Cui, Zhenru Zhang, Zhipeng Zhou, and Zihan
 650 Qiu. Qwen3 technical report, 2025. URL <https://arxiv.org/abs/2505.09388>.

651

652 Shunyu Yao, Jeffrey Zhao, Dian Yu, Nan Du, Izhak Shafran, Karthik Narasimhan, and Yuan Cao.
 653 React: Synergizing reasoning and acting in language models, 2023. URL <https://arxiv.org/abs/2210.03629>.

654

655 Qiying Yu, Zheng Zhang, Ruofei Zhu, Yufeng Yuan, Xiaochen Zuo, Yu Yue, Tiantian Fan, Gaohong
 656 Liu, Lingjun Liu, Xin Liu, Haibin Lin, Zhiqi Lin, Bole Ma, Guangming Sheng, Yuxuan Tong, Chi
 657 Zhang, Mofan Zhang, Wang Zhang, Hang Zhu, Jinhua Zhu, Jiaze Chen, Jiangjie Chen, Chengyi
 658 Wang, Hongli Yu, Weinan Dai, Yuxuan Song, Xiangpeng Wei, Hao Zhou, Jingjing Liu, Wei-Ying
 659 Ma, Ya-Qin Zhang, Lin Yan, Mu Qiao, Yonghui Wu, and Mingxuan Wang. Dapo: An open-source
 660 llm reinforcement learning system at scale, 2025. URL <https://arxiv.org/abs/2503.14476>.

661

662 Yang Yue, Zhiqi Chen, Rui Lu, Andrew Zhao, Zhaokai Wang, Yang Yue, Shiji Song, and Gao Huang.
 663 Does reinforcement learning really incentivize reasoning capacity in llms beyond the base model?,
 664 2025. URL <https://arxiv.org/abs/2504.13837>.

665

666 Lunjun Zhang, Arian Hosseini, Hritik Bansal, Mehran Kazemi, Aviral Kumar, and Rishabh Agarwal.
 667 Generative verifiers: Reward modeling as next-token prediction, 2025. URL <https://arxiv.org/abs/2408.15240>.

668

669

670

671

672

673

674

675

676

677

678

679

680

681

682

683

684

685

686

687

688

689

690

691

692

693

694

695

696

697

698

699

700

701

702 **A THE USE OF LARGE LANGUAGE MODELS**
703704 In preparing this manuscript, we used a large language model (LLM) solely for polishing the writing
705 style and improving the clarity of the manuscript. The LLM was not used for generating research
706 ideas, designing experiments, conducting analyses, or deriving results. All scientific contributions,
707 including the conceptualization, methodology, experiments, and conclusions, were developed entirely
708 by the authors.
709710 **B IMPLEMENTATION DETAILS**
711712 **B.1 HYPERPARAMETERS**
713714 Table 2 and Table 3 show the detailed hyperparameters we use during training and evaluation.
715716
717 **Table 2: RL Training Hyperparameters for ReVeal-Qwen2.5-32B-Instruct and ReVeal-DAPO-Qwen-32B**
718

| 719 Parameter | 720 Qwen2.5-32B-Instruct | 721 DAPO-Qwen-32B |
|----------------------------------|---------------------------------|--------------------------|
| 722 Max Turn | 723 3 | 724 3 |
| 725 Training Batch Size | 726 128 | 727 1024 |
| 728 Mini-Batch Size | 729 16 | 730 256 |
| 731 Learning Rate (Actor) | 732 5×10^{-7} | 733 1×10^{-6} |
| 734 Learning Rate (Critic) | 735 1×10^{-5} | 736 1×10^{-5} |
| 737 KL Coefficient | 738 0.0 | 739 0.0 |
| 740 Maximum Prompt Length | 741 4,096 | 742 4,096 |
| 743 Maximum Response Length | 744 8,192 | 745 12,288 |
| 746 Maximum Tool Response Length | 747 4,096 | 748 4,096 |
| 749 Temperature | 750 1.0 | 751 1.0 |
| 752 Training Epochs | 753 4 | 754 10 |

755 **Table 3: RL Evaluation Hyperparameters for Qwen2.5-32B-Instruct and DAPO-Qwen-32B**

| 756 Parameter | 757 Qwen2.5-32B-Instruct | 758 DAPO-Qwen-32B |
|----------------------------------|---------------------------------|--------------------------|
| 759 Maximum Prompt Length | 760 4,096 | 761 4,096 |
| 762 Maximum Response Length | 763 20,480 | 764 32,768 |
| 765 Maximum Tool Response Length | 766 4,096 | 767 4,096 |
| 768 Do Sample | 769 True | 770 True |
| 771 Temperature for Pass@1 | 772 0.6 | 773 0.6 |
| 774 Top_p for Pass@1 | 775 0.9 | 776 0.9 |
| 777 Rollout for Pass@1 | 778 10 | 779 10 |
| 780 Temperature for Pass@k | 781 0.6 | 782 0.6 |
| 783 Top_p for Pass@k | 784 0.9 | 785 0.9 |
| 786 Rollout for Pass@k | 787 128 | 788 128 |

789 **B.2 CASE STUDY OF REVEAL**
790791 Table 4 shows a detailed case of ReVeal.
792793 **B.3 PROMPT TEMPLATES**
794795 Table 5 shows the comparison between the commonly used Think-Answer prompt and our Generation-
796 Verification Prompt. Our prompt guides the model to continuously alternate between generation
797 and verification until the correct answer is obtained. Additionally, to enable the extraction of code
798 generated by the model for providing accurate training rewards, we instruct the model to enclose the
799 code within python blocks.
800

756

757

758

759

Table 4: Case Study of ReVeal Performing Iterative Generation and Verification

760 Question:

761 The Two-dimensional kingdom has a regular army of n people... The Two-dimensional kingdom has m vests at
 762 its disposal, the j -th vest's size equals b^j . Help mobilize the Two-dimensional kingdom's army: equip with vests
 763 as many soldiers as possible.

764 Response:**<generation-think>**

766 The problem can be solved using a dual circulation.
 767 Here's a step-by-step approach to the solution:

768 ...
 769 Wait, I can use a greedy approach to solve this problem. Let me try the greedy algorithm by following steps:
 770 ...

</generation-think>**<generation-answer>**

772 ```python
 773 def equip_soldiers(n, m, x, y, a, b):
 774 ...
 775 ...

</generation-answer>**<verification-think>**

777 Now, we will verify the code with the provided test cases.

778 - Example Input 1 should result in matching 2 pairs: (Soldier at index 1 with Vest at index 1) and (Soldier at
 779 index 3 with Vest at index 2). There is no possible matching for the remaining soldiers with the available vests
 780 within the given range.

780 Wait, I could add an extra test case for verification: more vests than soldiers...

</verification-think>**<verification-answer>**

782 - Input:
 783 ```1 3 5 ```
 784 - Expected Output:
 785 ```3 2 ```
 786 ...

</verification-answer>**<tool-feedback>**

788 ...
 789 - Actual Output:
 790 ```3 1 ```
 791 - Judgement:
 792 Failed

</tool-feedback>**<generation-think>**

796 The initial code provided did not successfully handle the actual output as expected. There is a discrepancy where
 797 the vest index tracked in the loop is not correctly being reset or updated...

798 Alternatively, I should create a list that keeps track of which vests have already been used and adjust the code
 799 logic to ensure each vest is used only once. Here is a revised version of the code:

800 ...
 801 </verification-answer>

<tool-feedback>

802 ...
 803 - Actual Output:
 804 ```3 2 ```
 805 - Judgement:
 806 Passed

</tool-feedback>

808

809

810

811

Table 5: Comparison Between Think-Answer Prompt and ReVeal Prompt

812

813

system

You are Qwen, created by Alibaba Cloud. You are a helpful assistant.

user

{question}

817

First think about the reasoning process in the mind and then provides the user with the answer. The reasoning process and answer are enclosed within `<think> </think>` and `<answer> </answer>` tags, respectively, i.e., `<think>` reasoning process here `</think>` `<answer>` answer here `</answer>`. Enclose your code within delimiters as follows.

```` python`

YOUR CODE HERE

`````**assistant**

823

824

825

826

827

828

829

830

831

832

833

834

B.4 TEMPLATES USED FOR TOOL FEEDBACK

835

836

837

Table 6 shows the mapping between execution results and hint templates: (1) for test cases that are verified as successful, we give a [Passed] signal in the judgement area; (2) for test cases that are verified as failed, we give a [Failed] signal in the judgement area; (3) for test cases that are verified as wrong, we give a clear feedback of [Wrong test case] for individual failures, or [No correct test cases generated] if all test cases are invalid; (4) for format error, we will give the feedback of formatting instructions to guide correct generation.

838

839

840

C THE EFFECTIVENESS OF SHORT-TERM MEMORY

841

842

843

844

845

To prevent the interaction context from growing unbounded and to keep inference efficient, we use a short-term memory mechanism. The system keeps a rolling window of the last three generation–verification turns and discards older interactions. For those retained turns, it preserves the full content of code, test cases, and tool feedback. This design allows the model to reuse information from recent history and build on previous attempts, which helps reduce redundant exploration and speed up convergence.

846

847

848

849

850

851

852

853

854

855

856

857

We compare models with and without memory integration. The baseline model without memory provides complete historical information from all previous turns directly to the model, maintaining full contextual details throughout the interaction sequence. We verified the impact of ReVeal on Pass@1 by LiveCodeBench with and without memory. Test results indicate that introducing short-term memory does not cause a decline in Pass@1 (w/o memory 38.2% vs. w/ memory 38.3% at turn 15), and may even yield a slight performance boost. This sustained improvement capability highlights the memory mechanism’s effectiveness in enabling continuous learning and adaptation within computational constraints.

864

865

866

Table 6: Tool Feedback Templates for Different Execution Result Types.

867

| Execution Results | Feedback |
|--------------------|---------------------------------------------------------------------------------------------------------------------------------------------------------------------------------------------------------------------------------------------------------------------------------------------------------------------------------------------------------------------------------------------------------------------------------------------------------------------------------------------------------------------------------------------------------------------------------------------------------------------------------------------------|
| | <ul style="list-style-type: none"> - Input: {input} |
| | <ul style="list-style-type: none"> - Expected Output: {expected output} |
| Success Test cases | <ul style="list-style-type: none"> - Actual Output: {actual output} - Judgement Passed |
| | <ul style="list-style-type: none"> - Input: {input} |
| | <ul style="list-style-type: none"> - Expected Output: {expected output} |
| Failed Test cases | <ul style="list-style-type: none"> - Actual Output: {actual output} - Judgement Failed - Failed Reason {failed reason} |
| | <ul style="list-style-type: none"> - Input: {input} |
| | <ul style="list-style-type: none"> - Expected Output: {expected output} |
| Wrong Test Cases | <ul style="list-style-type: none"> - Actual Output: {actual output} - Judgement Wrong test case. <p>No correct test cases are generated.</p> |
| Error Format | <p>No valid code because of the incorrect format. Write Python code again, and present the code in</p> <pre>```python Your code ```</pre> <p>within <generation-answer> </generation-answer> tags. After that, verify your code by generating test cases:</p> <ol style="list-style-type: none"> 1. Extract sample test cases if the problem description includes them... 2. Wrap each test case using the following format: <ul style="list-style-type: none"> - Input: ``` testcase input ``` - Expected Output: ``` expected testcase output ``` |

916

917

918 D MORE EXPERIMENTS ON QWEN2.5-32B-INSTRUCT
919

920 **Main Results.** To further validate the effectiveness and scalability of ReVeal across different base
921 models, we additionally conduct experiments on Qwen2.5-32B-Instruct. As shown in Table 7, ReVeal
922 achieves a 4.1% improvement in Pass@1 over the single-turn RL baseline. Moreover, using TAPO
923 with joint verifiable rewards yields higher Pass@1 compared to ReVeal with outcome-only reward,
924 while maintaining a higher $\Delta \uparrow$ and near-zero $\Delta \downarrow$. These results demonstrate that ReVeal remains
925 effective and stable across backbones of varying capability.

926 **Training Curves.** Figure 5 shows concurrent improvements in both code accuracy and test-case
927 accuracy when using TAPO with joint rewards, indicating that explicitly optimizing self-verification
928 leads to more reliable verification and drives stronger multi-turn refinement, echoing our main
929 findings on DAPO-Qwen-32B.

930 **Significance.** To demonstrate that the performance improvements are statistically significant, we
931 repeated the experiment 8 times and reported the $mean \pm std$ in Table 8, confirming the significance
932 of the gains.

933 Table 7: Performance comparison of ReVeal (Qwen2.5-32B-Instruct) with baseline methods on
934 LiveCodeBench. Pass@1 indicates the success rate; $\Delta \uparrow$ and $\Delta \downarrow$ represent the percentages of incorrect
935 solutions corrected and correct solutions degraded after revision, respectively.

| 936 Model | 937 LiveCodeBench V5 | | |
|---------------------------------------------------------------|-----------------------------|-------------------|---------------------|
| | 938 Pass@1 | $\Delta \uparrow$ | $\Delta \downarrow$ |
| <i>939 Existing Baselines</i> | | | |
| 940 Qwen2.5-32B-Instruct | 941 26.6 | - | - |
| 942 DAPO-Qwen2.5-32B | 943 29.6 | - | - |
| 944 Qwen2.5-Coder-32B-Instruct | 945 30.5 | - | - |
| 946 w/ critic $\times 5$ Qwen2.5-Coder | 947 29.6 | 2.14 | 3.04 |
| 948 w/ critic $\times 5$ GPT-4o | 949 32.9 | 4.82 | 2.50 |
| 950 w/ critic $\times 5$ CTRL | 951 33.4 | 3.75 | 0.89 |
| <i>952 RL based on Qwen2.5-32B-Instruct</i> | | | |
| 953 Single-turn RL | 954 33.9 | - | - |
| 955 ReVeal $\times 6$ | 956 38.0 | 3.41 | 0.0 |
| <i>957 Ablation Study: TAPO with Joint Verifiable Rewards</i> | | | |
| 958 ReVeal $\times 6$ w/ outcome reward | 959 37.1 | 2.98 | 0.0 |
| 960 ReVeal $\times 6$ w/ TAPO with joint rewards | 961 38.0 | 3.41 | 0.0 |

962 Table 8: Significance test of ReVeal (Qwen2.5-32B-Instruct) on LiveCodeBench V5. $mean \pm std$
963 indicates the average code pass@1 from 8 repeated experiments.

| 964 Model | 965 LiveCodeBench V5 | |
|-------------------------------------------------|-----------------------------|-----|
| | 966 $mean \pm std$ | 967 |
| 968 ReVeal $\times 6$ turn w/ turn-level reward | 969 38.02 \pm 0.43 | 970 |
| 971 ReVeal $\times 6$ turn w/ outcome reward | 972 37.09 \pm 0.33 | 973 |

974 E EXPERIMENTS ON QWEN3-4B-INSTRUCT
975

976 To cover models of different scales, we additionally evaluated ReVeal on smaller model Qwen3-4B-
977 instruct (Yang et al., 2025). The results on Table 9 show that ReVeal brings substantial performance
978 gains, far exceeding other baseline methods and enables deeper test-time scaling. This provides
979 further evidence that ReVeal is not tied to a single scale (32B) and can generalize across different
980 models.

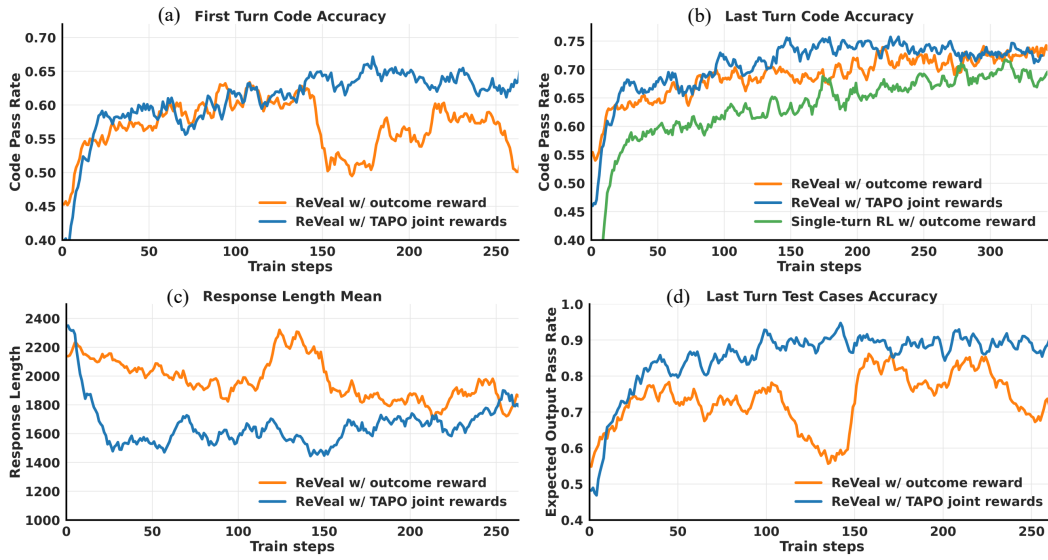


Figure 5: Comparison of code accuracy, test case accuracy, and response length across training for ReVeal (Qwen2.5-32B-Instruct) with turn-level rewards, ReVeal with outcome-only rewards, and single-turn RL without tool integration.

Table 9: Performance comparison of ReVeal trained based on Qwen3-4B-Instruct with different training turns. Pass@1 indicates the success rate.

| Model | LiveCodeBench V6 | | CodeContests | |
|---------------------------|------------------|--------|--------------|--------|
| | Pass@1 | Pass@1 | Pass@1 | Pass@1 |
| Qwen3-4B-Instruct | 33.1 | | 24.3 | |
| Single-turn RL | 39.0 | | 26.9 | |
| ReVeal (Max train turn=1) | | | | |
| ×1 turn | 37.3 | | 26.6 | |
| ×5 turn | 41.5 | | 30.6 | |
| ×8 turn | 41.7 | | 30.7 | |
| ReVeal (Max train turn=3) | | | | |
| ×1 turn | 40.6 | | 28.5 | |
| ×5 turn | 44.1 | | 33.6 | |
| ×8 turn | 44.5 | | 33.9 | |
| ReVeal (Max train turn=5) | | | | |
| ×1 turn | 38.6 | | 28.4 | |
| ×5 turn | 43.1 | | 33.2 | |
| ×8 turn | 44.0 | | 33.5 | |

F ABLATIONS: SEPARATING FRAMEWORK-LEVEL AND RL TRAINING GAINS

To disentangle the effect of the ReVeal multi-turn framework from the effect of ReVeal RL training, we evaluate several variants that progressively add components of ReVeal.

We first apply the ReVeal multi-turn framework to Qwen2.5-32B-Instruct without any RL training, using exactly the same ReVeal prompt format and code-execution tool. As shown in Table 10, this variant produces only modest gains and fails to sustain effective deep multi-turn refinement: performance improves slightly from 1 to 3 turns and then saturates or even drops. This indicates that simply changing the prompting scheme and enabling multi-turn tool feedback is not sufficient.

We then apply the same ReVeal multi-turn framework with code execution to stronger baselines such as DAPO-Qwen2.5-32B and Single-turn RL at test time, again without additional RL under the ReVeal objective, these multi-turn variants either exhibit gains in the first few turns and then begin to

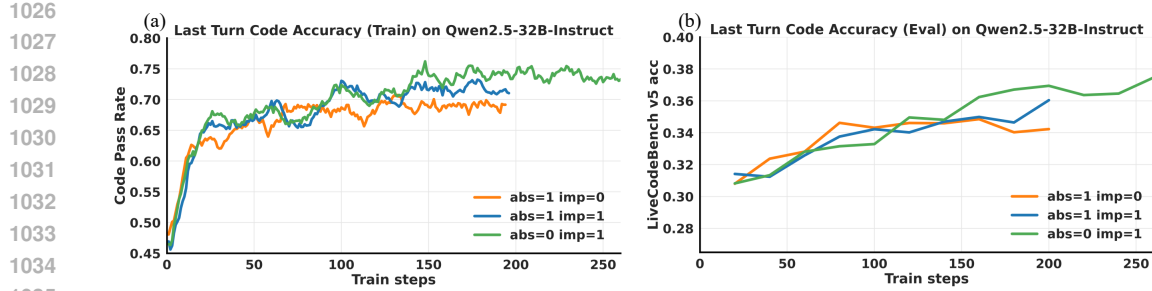


Figure 6: Effect of generation-reward coefficients (abs , imp) on ReVeal (Qwen2.5-32B-Instruct). We plot (a) training code accuracy and (b) LiveCodeBench v5 accuracy across training for three settings of: $(1, 0)$, $(1, 1)$, and $(0, 1)$.

degrade, or show almost no improvement at all (Table 11). While this confirms that most of ReVeal’s gains cannot be explained by multi-turn framework alone.

Finally, Table 11 reports two stronger ablations, ReVeal (no-gen RL) and ReVeal (no-ver RL), where we still use the ReVeal multi-turn framework but RL-train only one role: we pair a ReVeal-trained verifier with an untrained base generator (no-gen RL), or a ReVeal-trained generator with an untrained base verifier (no-ver RL). ReVeal (no-ver RL) yields gains in the first few turns but quickly saturates, whereas the full ReVeal model continues to improve with more turns and achieves higher Δ_{\uparrow} and lower Δ_{\downarrow} . This indicates that ReVeal’s explicit optimization of verification yields clear performance gains and enables deeper test-time scaling. ReVeal (no-gen RL) continues to improve with more turns even when paired with a relatively weak generator, suggesting that ReVeal’s explicit optimization of verification is key to enabling deeper test-time scaling. Taken together, these ablations indicate that while the multi-turn framework and tool feedback are helpful, the main gains come from explicitly training by ReVeal RL objective.

Table 10: Performance of Qwen2.5-32B-Instruct under the ReVeal multi-turn framework, with and without RL training. Pass@1 indicates the success rate; Δ_{\uparrow} and Δ_{\downarrow} represent the percentages of incorrect solutions corrected and correct solutions degraded after revision.

| Model | LiveCodeBench V5 | | |
|------------------------------------------|------------------|---------------------|-----------------------|
| | Pass@1 | Δ_{\uparrow} | Δ_{\downarrow} |
| ReVeal Multi-turn Framework w/o Training | | | |
| $\times 1$ turn | 26.3 | - | - |
| $\times 3$ turn | 27.5 | - | - |
| $\times 6$ turn | 27.4 | 2.40 | 1.31 |
| ReVeal Multi-turn Framework w/ Training | | | |
| $\times 1$ turn | 35.7 | - | - |
| $\times 3$ turn | 37.5 | - | - |
| $\times 6$ turn | 38.0 | 3.41 | 0.0 |

G TAPO REWARD ABLATIONS

TAPO Reward Ablations Besides the reward-signal ablation comparing ReVeal (outcome-only) variant with the full joint-reward in Table 1, we additionally include two ReVeal variants on top of the outcome-only baseline: ReVeal (outcome+gen) and ReVeal (outcome+ver). As shown in Table 12, both variants outperform the outcome-only version, and the full ReVeal achieves the overall best results. This indicates that both r_{gen} and r_{ver} make useful contributions beyond the outcome reward, with r_{gen} supervises both generation and verification by encouraging exposing more informative failure modes and larger subsequent code improvements, while r_{ver} supervises test case accuracy directly.

1080
 1081 Table 11: Performance on LiveCodeBench V6 for configurations designed to disentangle the gains
 1082 from the ReVeal multi-turn framework and from ReVeal RL training. We compare: (i) applying the
 1083 multi-turn framework to existing baselines without ReVeal RL, (ii) ReVeal variants where only the
 1084 generator or only the verifier is RL-trained (no-gen RL / no-ver RL), and (iii) full ReVeal with RL on
 1085 both roles.

| Configuration | LiveCodeBench V6 | | |
|------------------------------------------------------------------|------------------|---------------------|-----------------------|
| | Pass@1 | Δ_{\uparrow} | Δ_{\downarrow} |
| <i>Existing Baselines + ReVeal Multi-turn Framework</i> | | | |
| Base Model + ReVeal multi-turn framework | | | |
| ×1 turn | 28.4 | - | - |
| ×5 turn | 32.8 | 4.53 | 0.75 |
| ×8 turn | 31.8 | 4.15 | 1.70 |
| Single-turn RL model + ReVeal multi-turn framework | | | |
| ×1 turn | 33.4 | - | - |
| ×5 turn | 32.8 | 1.53 | 1.36 |
| ×8 turn | 33.0 | 2.05 | 1.53 |
| <i>ReVeal with RL on one role</i> | | | |
| ReVeal (no-gen RL): Base model as Generator + ReVeal as Verifier | | | |
| ×1 turn | 29.0 | - | - |
| ×5 turn | 33.6 | 6.16 | 0.91 |
| ×8 turn | 33.8 | 6.39 | 0.91 |
| ReVeal (no-ver RL): ReVeal as Generator + Base model as Verifier | | | |
| ×1 turn | 34.6 | - | - |
| ×5 turn | 36.9 | 2.94 | 0.53 |
| ×8 turn | 36.8 | 4.25 | 1.26 |
| <i>ReVeal with full RL training</i> | | | |
| ReVeal | | | |
| ×1 turn | 34.8 | - | - |
| ×5 turn | 37.2 | 3.71 | 0.0 |
| ×8 turn | 37.7 | 5.62 | 0.0 |

1112
 1113 **Generation-Reward Ablation** Our generation reward decomposes into an absolute term (abs,
 1114 the code accuracy at the current turn) and an improvement term (imp, how much the current turn’s
 1115 code accuracy improves over the previous turn). In our default setting, we use $\text{abs} = 0$ and $\text{imp} =$
 1116 1; that is, we only use the change in code pass rate to reward the quality of the generated tests and
 1117 the current-turn correction. In early experiments on Qwen2.5-32B-Instruct, we compared several
 1118 weightings ($\text{abs}/\text{imp} = 0/1, 1/1, 1/0$) and observed $0/1 > 1/1 > 1/0$ as shown in Figure 6, suggesting
 1119 that emphasizing improvement over absolute accuracy leads to better multi-turn performance.

H TRAINING-TURN COUNT ABLATION

1124 We vary the training horizon to 1, 3, and 5 turns while keeping other settings fixed. As shown in
 1125 Table 9, all ReVeal variants outperform the single-turn RL baseline; training with 3 turns yields much
 1126 larger gain than 1-turn training, while increasing the horizon further to 5 turns brings no additional
 1127 improvement, suggesting that the benefit saturates around 3-5 turns on our current (mostly solvable)
 1128 training set. On this training set, mean rewards can reach 4.5, which means most problems are already
 1129 solved within 3 generation-verification turns, so the additional 2 training turns provide limited extra
 1130 signal on a small fraction of very difficult questions. We expect longer training horizons to be more
 1131 beneficial on more challenging training data.

1132 Importantly, for all training horizons (1, 3, and 5), the corresponding models continue to improve
 1133 when we allow more inference turns than they were trained on, indicating that extrapolation beyond
 the training horizon is effective even when the model is trained with only a single turn.

1134
 1135 Table 12: Performance comparison of ReVeal trained based on DAPO-Qwen2.5-32B with different
 1136 verifiable rewards. Pass@1 indicates the success rate.

| Model | LiveCodeBench V6 | CodeContests |
|-------------------------------|------------------|--------------|
| | Pass@1 | Pass@1 |
| ReVeal (outcome only) | | |
| ×1 turn | 32.7 | 20.0 |
| ×5 turn | 35.9 | 26.1 |
| ×8 turn | 36.1 | 27.4 |
| ReVeal (outcome+ver) | | |
| ×1 turn | 32.3 | 17.3 |
| ×5 turn | 36.6 | 26.5 |
| ×8 turn | 36.8 | 27.8 |
| ReVeal (outcome+gen) | | |
| ×1 turn | 30.7 | 17.2 |
| ×5 turn | 37.1 | 26.6 |
| ×8 turn | 38.0 | 28.2 |
| ReVeal Full (outcome+gen+ver) | | |
| ×1 turn | 34.8 | 22.3 |
| ×5 turn | 37.2 | 28.1 |
| ×8 turn | 37.7 | 30.4 |

1155
 1156 Table 13: Performance comparison of ReVeal (DAPO-Qwen2.5-32B) with baseline methods on
 1157 HumanEval+ and MBPP+. Pass@1 indicates the success rate.

| Model | HumanEval+ | MBPP+ |
|-------------------------------------|-------------|-------------|
| | Pass@1 | Pass@1 |
| <i>Existing Baselines</i> | | |
| Qwen2.5-32B-Instruct | 85.4 | 75.4 |
| DAPO-Qwen2.5-32B | 86.0 | 73.8 |
| <i>RL based on DAPO-Qwen2.5-32B</i> | | |
| Single-turn RL | 86.0 | 76.2 |
| ReVeal×8 | | |
| ×1 turn | 85.2 | 77.9 |
| ×3 turn | 88.6 | 78.9 |
| ×4 turn | 88.4 | 78.9 |

I EVALUATION ON ADDITIONAL BENCHMARKS

1174 We evaluate ReVeal on two additional code-generation benchmarks: HumanEval+ (Liu et al., 2023)
 1175 and MBPP+ (Liu et al., 2023). The evaluation process follows the hyperparameter configuration
 1176 specified in Table 3. We use Pass@1 to measure the success rate of the model’s final code solutions.
 1177 Although these benchmarks differ from our training data, ReVeal still yields larger gains over the
 1178 baselines as shown in Table 13.

J GRADIENT-BASED INCENTIVE ANALYSIS FOR TAPO

1183 ReVeal’s multi-turn framework explicitly elicits verification turns in the trajectory, allowing veri-
 1184 fication tokens to be meaningfully optimized. Within this multi-turn framework, we analyze how
 1185 TAPO modifies the underlying PPO objective and gradients relative to an outcome-only baseline.
 1186 The analysis below shows that TAPO’s credit assignment strengthens the optimization signal for veri-
 1187 fication, which helps explain why ReVeal widens the verification–generation (V–G) asymmetry. We
 1188 then contrast TAPO with a naive token-level implementation that lacks turn-aware credit assignment,

1188 illustrating how such a scheme can suffer from misattributed credit and reward gaming, and how
 1189 TAPO’s design avoids these issues and promotes co-evolution of code and test quality.
 1190

1191 **Outcome-only PPO baseline.** Consider an outcome-only PPO baseline that uses only the scalar
 1192 outcome reward r_{outcome} from Eq. 1, with the same KL and entropy regularizers as Reveal. Ignoring
 1193 these shared regularizers, its objective is
 1194

$$1195 J_{\text{out}}(\theta) = \mathbb{E}_{\tau \sim \pi_\theta} [r_{\text{outcome}}(\tau)]. \quad (9)$$

1196 With the Monte Carlo return in Eq. 5 and our choice $\gamma = 1$, $\lambda = 1$, the token-level return for all
 1197 tokens before the end-of-sequence is
 1198

$$1199 R_t^{\text{out}} = r_{\text{outcome}}(\tau). \quad (10)$$

1200 Let V_t^{out} be the critic’s estimate trained to regress R_t^{out} , and define the corresponding advantages
 1201

$$1203 A_t^{\text{out}} = R_t^{\text{out}} - V_t^{\text{out}}. \quad (11)$$

1204 Denote by \mathcal{T}_{gen} and \mathcal{T}_{ver} the token indices belonging to generation and verification turns respectively.
 1205 Up to the usual PPO clipping and scaling factors, the actor gradients for the two roles can be written
 1206 as
 1207

$$1208 g_{\text{gen}}^{\text{base}}(\theta) \propto \mathbb{E} \left[\sum_{t \in \mathcal{T}_{\text{gen}}} A_t^{\text{out}} \nabla_\theta \log \pi_\theta(a_t | s_t) \right], \quad (12)$$

$$1211 g_{\text{ver}}^{\text{base}}(\theta) \propto \mathbb{E} \left[\sum_{t \in \mathcal{T}_{\text{ver}}} A_t^{\text{out}} \nabla_\theta \log \pi_\theta(a_t | s_t) \right]. \quad (13)$$

1213 Thus, in the outcome-only baseline both generation and verification tokens are trained only through
 1214 the same outcome-based advantage.
 1215

1216 **TAPO-augmented objective and gradients.** TAPO augments the outcome objective with the
 1217 generation and verification rewards:
 1218

$$1219 J_{\text{TAPO}}(\theta) = \mathbb{E}_{\tau \sim \pi_\theta} \left[r_{\text{outcome}}(\tau) + \sum_k r_{\text{gen}}^k(\tau) + \sum_k r_{\text{ver}}^k(\tau) \right], \quad (14)$$

1222 where r_{gen}^k is the pass-rate based reward at generation turn k and r_{ver}^k is the test-quality reward at
 1223 verification turn k . TAPO routes these rewards to tokens through the turn-level return in Eq. 6 and
 1224 the combined return in Eq. 8. Following Eq. 8, we write the TAPO return and advantages as
 1225

$$1226 \tilde{R}_t = R_t + R_t^{\text{turn}}, \quad A_t^{\text{TAPO}} = \tilde{R}_t - V_t^{\text{TAPO}}, \quad (15)$$

1228 where V_t^{TAPO} is the critic trained to regress \tilde{R}_t . Using Eq. 6 together with the fact that $R_t = r_{\text{outcome}}$
 1229 for all tokens before EOS, we obtain explicit forms for the TAPO return. For a token t belonging to
 1230 generation turn k ,

$$1231 R_t^{\text{turn}} = r_{\text{gen}}^k, \quad \tilde{R}_t = r_{\text{outcome}} + r_{\text{gen}}^k. \quad (16)$$

1233 For a token t belonging to verification turn k , whose successor turn $k+1$ is generation, Eq. 6 gives

$$1234 R_t^{\text{turn}} = r_{\text{ver}}^k + r_{\text{gen}}^{k+1}, \quad \tilde{R}_t = r_{\text{outcome}} + r_{\text{ver}}^k + r_{\text{gen}}^{k+1}. \quad (17)$$

1236 The corresponding actor gradients under TAPO are
 1237

$$1238 g_{\text{gen}}^{\text{TAPO}}(\theta) \propto \mathbb{E} \left[\sum_{t \in \mathcal{T}_{\text{gen}}} A_t^{\text{TAPO}} \nabla_\theta \log \pi_\theta(a_t | s_t) \right], \quad (18)$$

$$1241 g_{\text{ver}}^{\text{TAPO}}(\theta) \propto \mathbb{E} \left[\sum_{t \in \mathcal{T}_{\text{ver}}} A_t^{\text{TAPO}} \nabla_\theta \log \pi_\theta(a_t | s_t) \right]. \quad (19)$$

1242 **Incremental gradients and widened V-G asymmetry.** To make the difference to the outcome-only
 1243 baseline explicit, we define the incremental gradients
 1244

$$1245 \quad \Delta g_{\text{gen}}(\theta) \propto \mathbb{E} \left[\sum_{t \in \mathcal{T}_{\text{gen}}} (A_t^{\text{TAPO}} - A_t^{\text{out}}) \nabla_{\theta} \log \pi_{\theta}(a_t | s_t) \right], \quad (20)$$

$$1247 \quad \Delta g_{\text{ver}}(\theta) \propto \mathbb{E} \left[\sum_{t \in \mathcal{T}_{\text{ver}}} (A_t^{\text{TAPO}} - A_t^{\text{out}}) \nabla_{\theta} \log \pi_{\theta}(a_t | s_t) \right], \quad (21)$$

1250 so that

$$1251 \quad g_{\text{gen}}^{\text{TAPO}}(\theta) = g_{\text{gen}}^{\text{base}}(\theta) + \Delta g_{\text{gen}}(\theta), \quad g_{\text{ver}}^{\text{TAPO}}(\theta) = g_{\text{ver}}^{\text{base}}(\theta) + \Delta g_{\text{ver}}(\theta). \quad (22)$$

1252 Using the definitions above we can write

$$1254 \quad A_t^{\text{TAPO}} - A_t^{\text{out}} = (\tilde{R}_t - V_t^{\text{TAPO}}) - (R_t^{\text{out}} - V_t^{\text{out}}) = R_t^{\text{turn}} - (V_t^{\text{TAPO}} - V_t^{\text{out}}). \quad (23)$$

1256 In the actor update, the critic outputs V_t are treated as baselines and are not differentiated with respect
 1257 to θ . Thus the additional actor gradients Δg_{gen} and Δg_{ver} are driven by the turn-level returns R_t^{turn}
 1258 that TAPO introduces.

1259 For generation tokens, $R_t^{\text{turn}} = r_{\text{gen}}^k$ depends only on the per-turn code pass-rate signal and does
 1260 not involve the verification reward. Relative to outcome-only PPO, TAPO therefore provides finer,
 1261 outcome-aligned signals for generation by decomposing changes in pass rate into turn-level contribu-
 1262 tions; this can be viewed as process-level reward shaping rather than introducing a new objec-
 1263 tive beyond code quality. For verification tokens, in contrast, $R_t^{\text{turn}} = r_{\text{ver}}^k + r_{\text{gen}}^{k+1}$ combines two
 1264 environment-grounded signals: test quality on the golden code and the effect of these tests on the
 1265 next generation turn. The outcome-only baseline optimizes verification tokens only through signals
 1266 mediated by final code quality, whereas TAPO adds verification-specific gradient components that
 1267 directly reward constructing high-quality, informative tests.

1268 Thus, on the one hand, ReVeal’s multi-turn framework explicitly elicits verification turns in the
 1269 trajectory, allowing verification tokens to be meaningfully optimized, which is not guaranteed by
 1270 other baseline methods. On the other hand, relative to outcome-only PPO, TAPO strictly enriches
 1271 the task-aligned reward signals: it explicitly optimizes the verification objective while leaving the
 1272 generation objective essentially unchanged up to finer credit assignment. This structural asymmetry
 1273 in the incremental gradients provides a gradient-level explanation for our empirical finding that TAPO
 1274 substantially increases verification accuracy and widens the V-G gap compared to other baselines.

1275 **Accurate turn-aware credit assignment and robustness to reward gaming.** A naive token-
 1276 level implementation for multi-turn generation–verification would simply attach each reward r_{gen}^k
 1277 or r_{ver}^k to the last token of the corresponding turn and then use a standard Monte Carlo return for
 1278 all earlier tokens in the trajectory, without the turn-aware routing in Eq. 6–8. This would propagate
 1279 the verification reward r_{ver}^k back through all preceding generation tokens and introduce gradient
 1280 terms of the form $r_{\text{ver}}^k \nabla_{\theta} \log \pi_{\theta}(a_t^{\text{gen}} | s_t^{\text{gen}})$ for tokens that do not causally influence r_{ver}^k , since r_{ver}^k is
 1281 evaluated on the golden code. Code tokens would then be updated by a signal they do not influence
 1282 (e.g., wrong code but strong tests still giving high verification reward to the code, or correct code but
 1283 weak tests inducing low verification reward), and the policy may learn spurious correlations between
 1284 code patterns and high test accuracy rather than improving true code quality.

1285 By contrast, TAPO’s reward design enforces accurate turn-level credit assignment, which is crucial
 1286 for stable and effective RL training. Its turn-level routing ensures that generation tokens are rewarded
 1287 only via outcome and pass-rate improvements (r_{outcome} and r_{gen}^k), and that verification tokens are
 1288 rewarded only when their tests are both strong on the golden code r_{ver}^k and helpful for subsequent
 1289 code refinement r_{gen}^{k+1} and r_{outcome} . Together with the shared policy for both roles, this structure
 1290 encourages co-evolution of code and tests: better tests expose more informative failure modes and
 1291 increase r_{gen}^k and r_{outcome} , while better code raises the bar for verification and encourages tests that
 1292 achieve higher r_{ver}^k .

1294 The same credit-assignment pattern naturally extends to more general generation–verification designs
 1295 with task-specific verification rewards, while remaining robust and compatible across different tasks.
 1296 For example, if a verification turn were rewarded for judging correctness, the naive implementation

1296 mentioned above could lead to collusion between generation and verification: generation might
1297 collapse to trivially wrong solutions that are extremely easy for verification to flag as incorrect,
1298 allowing verification to obtain high verification reward while the solution quality remains poor.
1299 TAPO’s separation of roles prevent such self-referential reward exploitation and make the ReVeal
1300 training paradigm robust across different verification reward designs.
1301

1302 K LIMITATIONS

1303

1304 Our current instantiation of ReVeal is primarily optimized for functional correctness: solutions
1305 that produce correct outputs on the available golden tests are treated as correct, and violations of
1306 time/space complexity are only penalized when they cause failures under these tests (e.g., timeouts
1307 within the execution budget). As a result, brute-force or computationally inefficient solutions that
1308 still pass all golden tests may not be distinguished from truly efficient ones. A natural direction for
1309 future work is to add stress tests with very large inputs; these test cases can then be used to compute
1310 the outcome and generation rewards, directly encouraging solutions that remain correct under stricter
1311 time/space constraints. Another complementary direction is to enrich the tool interface with runtime
1312 and resource statistics (e.g., execution time, memory usage) and incorporate these signals into the
1313 outcome, generation, and verification rewards, encouraging both efficient code and stress test cases
1314 that reliably expose inefficient solutions.
1315
1316
1317
1318
1319
1320
1321
1322
1323
1324
1325
1326
1327
1328
1329
1330
1331
1332
1333
1334
1335
1336
1337
1338
1339
1340
1341
1342
1343
1344
1345
1346
1347
1348
1349